TJVS Turkish Journal of Vascular Surgery

Turk J Vasc Surg.2026;35(1):60-7
DOI: 10.9739/tjvs.2025.12.073

Available online at www.turkishjournalofvascularsurgery.org

Original Article

The assessment of the effects of dexmedetomidine on the ischemia-reperfusion injury to the lower extremity skeletal muscles in a ruptured abdominal aortic aneurysm model

Ibrahim Yel[1], Sedat Ozan Karakisi[1], Dogus Hemsinli[1], Saban Ergene[1], Tolga Mercantepe[2], Levent Tumkaya[2], Adnan Yilmaz[3]

[1]Recep Tayyip Erdoğan University, Faculty of Medicine, Department of Cardiovascular Surgery, Rize, Türkiye
[2]Recep Tayyip Erdoğan University, Faculty of Medicine, Department of Histology and Embryology, Rize, Türkiye
[3]Recep Tayyip Erdoğan University, Faculty of Medicine, Department of Medical Biochemistry, Rize, Türkiye

Received: December 28, 2025 Accepted: February 24, 2026 Published online: March 06, 2026

Abstract

Aim: This study aimed to evaluate the effects of dexmedetomidine (Dex), commonly used during the intensive care process—particularly in the postoperative period due to its analgesic and sedative properties— on lower extremity skeletal muscle ischemia–reperfusion injury (IRI) in an experimental ruptured abdominal aortic aneurysm (RAAA) rat model.

Material and Methods: Twenty-four male Sprague Dawley rats (3–4 months old; mean weight 244±32 g) were randomly allocated into three groups: SHAM, IRI, and ischemia–reperfusion injury treated with intraperitoneal 100mcg/kg dexmedetomidine (IRI&Dex). An experimental RAAA model was established in all groups. Lower extremity skeletal muscle tissues were harvested and evaluated using histopathological, immunohistochemical, and biochemical analyses.

Results: Light microscopic examination revealed normal myofibrillar architecture with typical nuclei in the SHAM group, widespread necrotic myofibrils with pyknotic nuclei in the IRI group, and predominantly preserved myofibrillar structures with occasional necrosis in the IRI&Dex group. Immunohistochemical analysis demonstrated dense actin and myosin positivity in the SHAM group, a marked reduction in the IRI group, and a significant increase in the IRI&Dex group compared to the IRI group. Caspase-3 expression was normal in the SHAM group, elevated in the IRI group, and near to normal in the IRI&Dex group. Biochemical analyses showed decreased glutathione (GSH) and increased malondialdehyde (MDA) levels in the IRI group, whereas Dex treatment significantly increased GSH and reduced MDA levels compared to the IRI group.

Conclusion: Histopathological, immunohistochemical, and biochemical findings indicate that dexmedetomidine markedly attenuates ischemia–reperfusion injury in lower extremity skeletal muscle in a rat model of ruptured abdominal aortic aneurysm.

Keywords: Ischemia-reperfusion, dexmedetomidine, skeletal muscle

INTRODUCTION

Ruptured abdominal aortic aneurysm (RAAA) constitutes a life-threatening vascular emergency and is associated with substantial perioperative mortality despite advances in surgical and anesthetic management [1]. In the absence of prompt surgical intervention, most patients succumb to massive hemorrhage and hemorrhagic shock. Even following surgical repair, mortality remains high, primarily due to complications such as myocardial infarction, respiratory failure, acute kidney injury, and multiple organ dysfunction [2].

CITATION

Yel I, Karakisi SO, Hemsinli D, Ergene S, Mercantepe T, Tumkaya L, et al. The assessment of the effects of dexmedetomidine on the ischemia-reperfusion injury to the lower extremity skeletal muscles in a ruptured abdominal aortic aneurysm model. Turk J Vasc Surg.2026;35(1):60-7.

Corresponding Author: Ibrahim Yel, Recep Tayyip Erdoğan University, Faculty of Medicine, Department of Cardiovascular Surgery, Rize, Türkiye
Email: ibrahim.yel@erdogan.edu.tr

The underlying pathophysiology of RAAA is multifactorial and includes profound hemorrhagic shock, systemic hypoperfusion, lower body ischemia caused by aortic cross-clamping during surgery, and subsequent ischemia–reperfusion injury (IRI) following clamp release. In patients presenting with hemodynamic instability, prolonged aortic clamping further exacerbates ischemic damage, while reperfusion initiates a cascade of inflammatory and oxidative processes that contribute to both local and remote organ injury [3]. Under physiological conditions, restoration of oxygen and nutrient delivery to ischemic tissues is sufficient to promote cellular recovery. However, prolonged ischemia alters mitochondrial function and antioxidant defense mechanisms, rendering tissues vulnerable to oxidative stress upon reperfusion. Excessive generation of reactive oxygen species (ROS) during reperfusion leads to lipid peroxidation, protein degradation, and irreversible cellular damage [4]. In addition to oxidative stress, increased intracellular calcium levels activate phospholipases and proteases, triggering apoptotic signaling pathways [5]. Activation of caspase-3 represents a critical and irreversible step in the execution phase of apoptosis [6].

Another key mechanism of IRI involves inflammatory cell infiltration of previously ischemic tissues following reperfusion. Neutrophil activation, complement system engagement, and increased endothelial permeability further amplify tissue injury. Simultaneously, impaired mitochondrial clearance of ROS results in sustained oxidative damage, particularly in skeletal muscle, which possesses a large ischemic burden during lower body hypoperfusion [7].

Lipid peroxidation markers, such as malondialdehyde (MDA), increase in parallel with oxidative stress, whereas antioxidant components, including glutathione (GSH) and glutathione peroxidase, are depleted during ischemia–reperfusion [8,9]. Therapeutic strategies targeting oxidative stress and apoptosis have therefore gained increasing attention in the prevention of IRI.

Dexmedetomidine (Dex), a selective α2-adrenergic receptor agonist widely used for its sedative and analgesic properties in perioperative and intensive care settings, has demonstrated antioxidant, antiinflammatory, and anti-apoptotic effects in various experimental and clinical models of IRI [10–12]. To the best of our knowledge, there are no studies in the literature specifically investigating lower extremity skeletal muscle ischemia–reperfusion injury associated with aortic cross-clamping in the setting of ruptured abdominal aortic aneurysm.

Accordingly, the present study aimed to investigate the effects of Dex on ischemia–reperfusion injury in lower extremity skeletal muscle using an experimental ruptured abdominal aortic aneurysm model in rats, with histopathological, immunohistochemical, and biochemical assessments.

MATERIAL AND METHODS

The animals used in this study were obtained from the Experimental Animals Application and Research Center of Recep Tayyip Erdoğan University. This study was conducted in accordance with the ARRIVE guidelines and approved by the Recep Tayyip Erdoğan University Animal Experiments Local Ethics Committee (Approval No: 2020/21, dated May 29, 2020). All experimental procedures were carried out at the Recep Tayyip Erdoğan University Experimental Animals Application and Research Center. All animals were housed under standard laboratory conditions, closely monitored, and provided with appropriate care throughout the experimental period at this facility.

Experimental animals

Thomas Lindsay's "ruptured abdominal aortic aneurysm model in rats" was used in this study. The shock to be applied within the scope of the model was determined according to ischemia and reperfusion times [13]. The study sample consisted of 24 Sprague Dawley male rats, 3-4 months old, weighing 244±32 g. These rats were divided into three groups: the SHAM group, the group in which ischemia-reperfusion injury will be induced -IRI group-, and the group in which IRI will be induced and treated with intraperitoneal Dex -IRI&Dex group-. The experiment protocol was initiated by giving anesthesia [10 ml/kg intramuscular (IM) Xylazine and 50 mg/kg IM Ketamine] to the standard experimental animals after 12-hour fasting.

Catheterization Phase: Catheterization was performed routinely in both IRI and IRI&Dex groups. The right carotid artery was surgically explored to allow arterial pressure monitoring, and the left internal jugular vein was surgically explored and cannulated with a 22G branul for blood and fluid administration. Additionally, the arterial line was monitored with a three-way tap and transducer set, and invasive pressure monitoring was performed throughout the experiment.

Shock Application Phase: The shock application phase in the model simulates aneurysm rupture and hemorrhagic shock. Within the scope of the model, it was decided to apply the shock for 60 minutes. When the catheterization process was completed, the subjects in both IRI and IRI&Dex groups were allowed to go into shock by taking blood from their carotid arteries into syringes containing 500 international units (IU) of heparin until mean arterial pressure (MAP) reached ≤50 mmHg. The blood samples were kept at room temperature so that they could be used in resuscitation. Once the MAP was ≤50mmHg, the shock application was continued for one hour. During this process, blood was retaken at regular intervals when necessary to ensure that the MAP was ≤50 mmHg.

Laparotomy + Ischemia + Resuscitation Phase: At the end of the shock application phase, the abdominal aorta was

reached through median laparotomy. After the exploration stage, anticoagulation was achieved by administering 100 IU intravenous (IV) heparin to all subjects. At the end of the 1-hour shock application phase, bulldog clamps were applied to all subjects in two regions, proximal to the superior mesenteric artery and at the level of the aortic bifurcation and the ischemia process was initiated. As soon as the clamps were placed, resuscitation was initiated, and half of the blood taken from the subjects and kept at room temperature was given back through internal jugular vein. The ischemia process in the model simulates surgical treatment, that is, stopping bleeding with aortic clamping and surgical reconstruction.

Drug Administration Phase: At the 30th minute of one-hour ischemia, 2 ml physiological saline was administered intraperitoneally to the subjects in the SHAM group, and 100 mcg/kg dexmedetomidine was administered to the subjects in the experimental groups by the same route [14].

Reperfusion Phase: In all subjects, after a one-hour ischemic period, the aortic clamps were opened, lower body ischemia was terminated, and the reperfusion process was initiated. The remaining blood was given back to the subjects immediately before the clamps were opened. The subjects were left in reperfusion for 120 minutes. Meanwhile, the subjects were given Ringer's lactate solution, replacing fluids so the MAP was>100 mmHg.

Experiment Termination Phase: At the end of the 120-minute reperfusion period, all subjects were euthanized by taking blood. During the entire experiment process, each subject's MAP values and heart rates were checked at 10-minute intervals.

Histological Tissue Follow-up Procedures

Sections of skeletal muscle tissue removed from rats were fixed in 10% formalin solution for 36 hours. Skeletal muscle tissue samples taken for histological evaluation were placed in tissue embedding cassettes and monitored on a tissue processor (ThermoScientific™ Citadel 2000). Tissues were dehydrated by subjecting them to 50%, 60%, 70%, 80%, 96%, and 100% alcohol solutions twice, respectively. Afterward, the tissues were kept in xylene and substitutes to clear them of dehydration agents in order to achieve transparency. Finally, the tissues were fixated in paraffin-filled chambers for paraffin embedding.

Following the tissue follow-up procedures, skeletal muscle tissue samples were blocked out with hard paraffin using a paraffin embedding device (Leica EG 1150 H). Then, a series of 4-5 µm thick sections were taken from the paraffin blocks using a rotary microtome (Leica RM2255). These sections were placed on adhesive and positively charged slides (Superior Marienfeld Histobond+).

Hematoxylin and Eosin Staining

4- 5 µm thick sections taken from paraffin blocks were stained with hematoxylin and eosin (H&E) using a staining device (Leica ST5020) in order first to evaluate the general histopathological appearance of the tissues.

Immunohistochemical Staining Protocol

2-3 µm thick sections taken from skeletal muscle tissues were incubated with actin primary antibody (ab184705, Abcam, UK), myosin primary antibody (ab184705, Abcam, UK) and caspase-3 primary antibodies (ab2242715, Abcam, UK), and appropriate secondary antibodies using the IHC (immunohistochemistry)/ ISH (In situ hybridization) device (Bond Max, LeicaBiosystems, Australia) after the deparaffinization phase. Thirty different areas in each section taken from each rat were evaluated by two histopathologists blinded to the study groups.

Measurement of MDA and GSH Levels

Lower extremity skeletal muscle samples were rapidly excised at the end of the experiment, rinsed with cold saline, and processed on ice. Approximately 50–100 mg of tissue was homogenized in 1.15% KCl solution at a ratio of 1:9 (w/v). The homogenates were centrifuged at 10.000 × g for 15 minutes at 4°C, and the supernatants were collected for biochemical analyses.

MDA measurement: MDA levels, as an indicator of lipid peroxidation, were determined using the thiobarbituric acid reactive substances (TBARS) method. Supernatant samples were mixed with thiobarbituric acid (TBA) reagent under acidic conditions and incubated at 95°C for 45 minutes to allow formation of the MDA–TBA adduct. After cooling and centrifugation, the absorbance of the supernatants was measured spectrophotometrically at 532 nm. A calibration curve was generated using malondialdehyde bis(dimethyl acetal), which was hydrolyzed under acidic conditions to yield free MDA. MDA concentrations were calculated from the standard curve and expressed as µmol/g tissue.

GSH measurement: Reduced glutathione (GSH) levels were determined using the 5.5′-dithiobis-(2- nitrobenzoic acid) (DTNB; Ellman reagent) method. Supernatant samples were treated with an appropriate protein-precipitating agent and centrifuged to obtain a clear supernatant. The resulting supernatant was reacted with DTNB in phosphate buffer, and the absorbance of the yellow-colored product was measured at 412 nm. GSH concentrations were calculated using a standard curve and expressed as µmol/g tissue. All biochemical analyses were performed and evaluated by a biochemistry specialist.

Statistical Analysis

The statistical analyses of the collected data were conducted using the SPSS Statistics 18.0 (Predictive Analytics Software Statistics for Windows, Version 18.0, SPSS Inc., Chicago, IL,

U.S., 2009) software package. Non-parametric data obtained from the semi-quantitative analyses were expressed as median with 25% and 75% percentiles, along with maximum and minimum values. After analyzing the differences between the groups using the non-parametric Kruskal-Wallis test followed by Tamhane's T2 test, the numerical data of the groups were analyzed. Probability (p) statistics of ≤0.05 were deemed to indicate statistical significance.

RESULTS

Histopathological Analysis

Light microscopic analysis of skeletal muscle sections showed myofibrils with normal nuclear morphology in the SHAM group (Figures 1A & 1B). The IRI group demonstrated diffuse necrotic myofibrils characterized by pyknotic nuclei (Figures 1C & 1D, Table 1). In the IRI&Dex group, myofibrils with normal nuclei were predominantly observed, together with occasional necrotic myofibrils (Figures 1E & 1F, Table 1).

Table 1. Semi-quantitative analysis

Score	Result
0	Less than 5%
1	Between 6% and 25%
2	Between 26% and 50%
3	More than 50%

Semi-quantitative scoring system used for immunohistochemical evaluation. Scores were assigned based on the percentage of positive staining

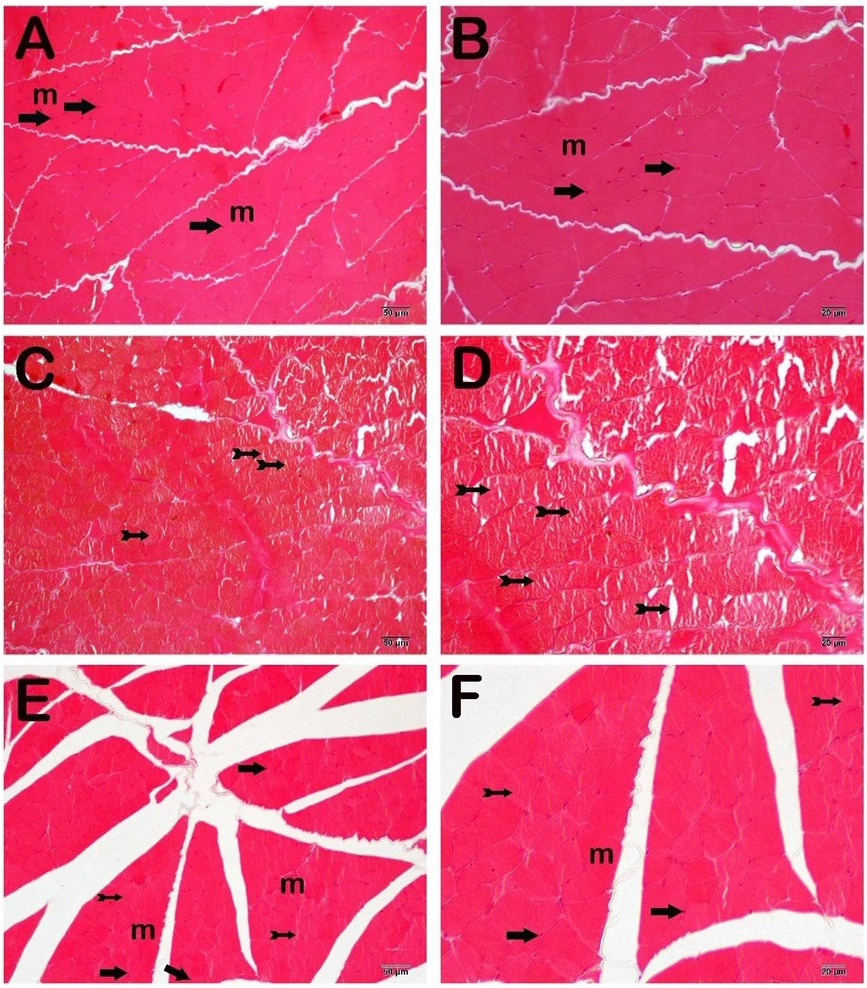

Figure 1. Representative light microscopic images of H&E-stained skeletal muscle sections. A(x20)-B(x40): myofibrils (m) with typical nuclei (arrow) can be observed in the skeletal muscle sections of the control group. C(x20)-D(x40): acute focal necrotic myofibrils (tailed arrow) can be observed in the skeletal muscle sections of the IRI group. E(x20)-F(x40): diffuse myofibrils with typical nuclei (arrow) and occasional necrotic myofibrils (tailed arrow) can be observed in the skeletal muscle sections of the IRI&Dex group

Immunohistochemical Analysis

Actin Primary Antibody

Light microscopic analysis of skeletal muscle sections incubated with an actin primary antibody revealed dense actin-positive myofibrils. In the IRI group, a marked reduction in actin positivity within the myofibrils was observed. In contrast, the IRI&Dex group demonstrated an increased number of actin-positive myofibrils in skeletal muscle sections compared with the IRI group (Figure 2, Table 2).

Myosin Primary Antibody

Light microscopic examination of skeletal muscle sections incubated with a myosin primary antibody demonstrated diffuse myosin-positive myofibrils in the SHAM group. Myosin positivity was reduced in the IRI group compared with the SHAM group, whereas the IRI&Dex group exhibited an increased number of myosin-positive myofibrils relative to the IRI group (Figure 3, Table 2).

Caspase-3 Primary Antibody

Light microscopic examination of skeletal muscle sections incubated with a caspase-3 antibody demonstrated myofibrils with normal nuclear morphology in the SHAM group. IRI group showed increased caspase-3 positivity in apoptotic myofibrils compared with the SHAM group. In contrast, the IRI&Dex group exhibited a reduced number of caspase-3–positive myofibrils relative to the IRI group (Figure 4, Table 2).

Figure 2. Representative light microscopic images of skeletal muscle incubated with actin primary antibody. A(x40): myofibrils with typical nuclei showing intense actin positivity (arrow) can be observed in the skeletal muscle sections of the control group [actin positivity score: 3(2.5-3)]. B(x40): decreased actin positivity can be observed in the skeletal muscle sections of the IRI group [actin positivity score: 1(0.5-1)]. C(x40): Actin-positive myofibrils can be observed in the skeletal muscle sections of the IRI&Dex group [actin positivity score: 2(1-2)] (Table 1)

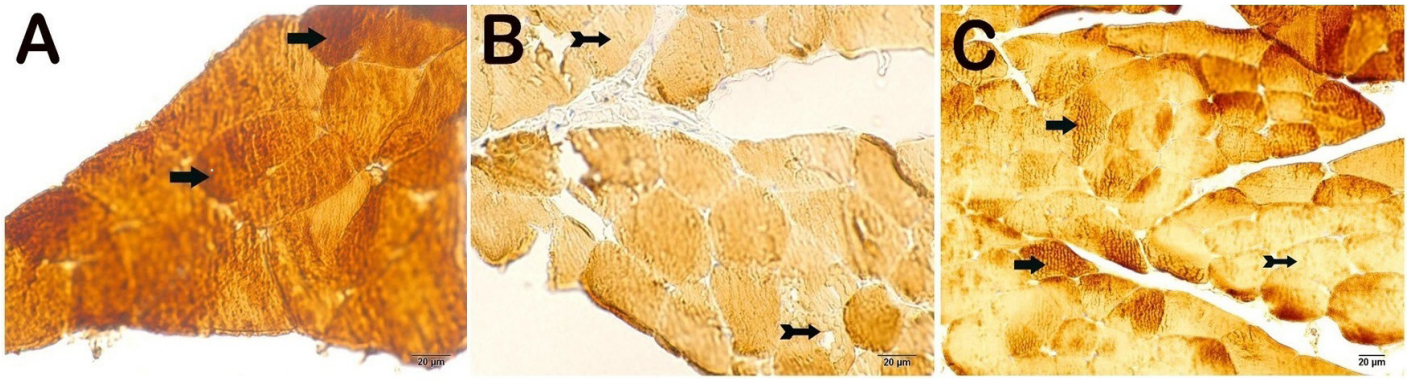

Figure 3. Representative light microscopic images of skeletal muscle sections incubated with myosin primary antibody. A(x40): myofibrils with typical nuclei showing intense myosin positivity (arrow) can be observed in the skeletal muscle sections of the control group [myosin positivity score: 3(3-3)]. B(x40): decreased myosin positivity can be observed in the skeletal muscle sections of the IRI group [myosin positivity score: 1(1-1.5)]. C(x40): Actin-positive myofibrils can be observed in the skeletal muscle sections of the IRI&Dex group [myosin positivity score: 2(2-2)] (Table 1)

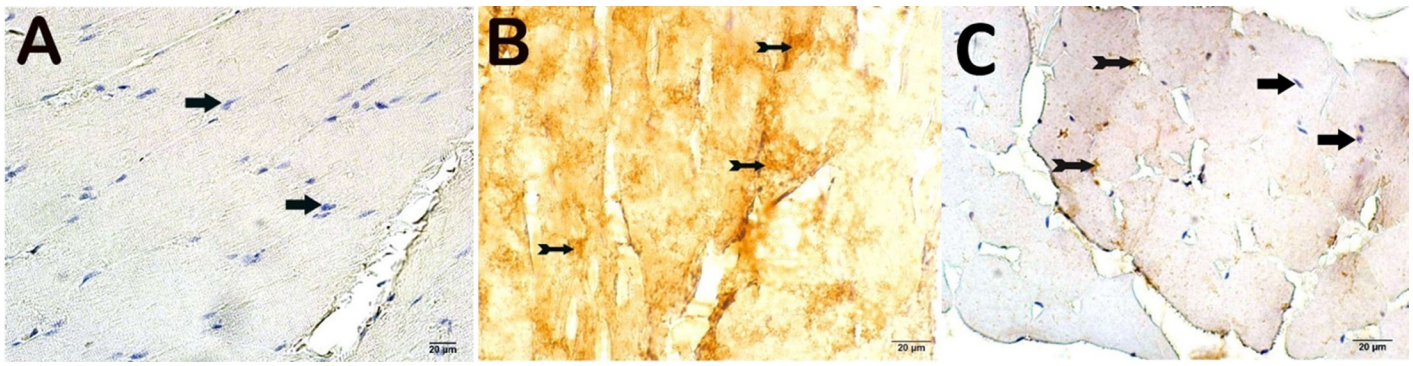

Figure 4. Representative light microscopic images of skeletal muscle incubated with caspase-3 antibody. A(x40): myofibrils with typical nuclei (arrow) can be observed in the skeletal muscle sections of the control group [caspase-3 positivity score: 0(0-0.5)]. B(x40): caspase-3 positive apoptotic myofibrils can be observed in the skeletal muscle sections of the IRI group [caspase-3 positivity score: 2(2-2)]. C(x40): myofibrils with typical nuclei can be observed in the skeletal muscle sections of the IRI&Dex group [caspase-3 positivity score: 1(1-1)] (Table 1)

Table 2. Immunohistochemical analysis results (median 25%-75% percentiles)

Group	Actin Positivity Score	Myosin Positivity Score	Caspase-3 Positivity Score
SHAM	3 (2.5-3)	3 (3-3)	0 (0-0.5)
IRI	1 (0.5-1)[a]	1 (1-1.5)[a]	2 (2-2)[a]
IRI&Dex	2 (1-2)[b,c]	2 (2-2)[d,e]	1 (1-1)[g,f]

Values are presented as median (25–75 percentiles). Actin and myosin positivity scores were significantly reduced in the ischemia–reperfusion injury (IRI) group compared with the SHAM group, whereas dexmedetomidine treatment resulted in a significant increase in actin and myosin positivity compared with the IRI group. Caspase-3 positivity was significantly increased in the IRI group and significantly decreased in the IRI + dexmedetomidine group. Statistical analysis was performed using the Kruskal–Wallis test followed by Tamhane's T2 post hoc test. a p: 0.000, compared with the SHAM group, b p: 0.017, compared with the SHAM group, c p: 0.001, compared with the IRI group, d p: 0.007, compared with the SHAM group, e p: 0.031, compared with the IRI group, f p: 0.029, compared with the SHAM group, g p: 0.007, compared with the IRI group

Biochemical Analysis

MDA levels

Biochemical analysis of the MDA levels of the skeletal tissue revealed that the MDA level was significantly increased in the IRI group compared to the SHAM group and that the MDA level was significantly decreased in the IRI&Dex group compared to the IRI group (Table 3).

GSH levels

Biochemical analysis of the GSH levels of the skeletal tissue revealed that the GSH level was significantly decreased in the IRI group compared to the SHAM group and that the GSH level was significantly increased in the IRI&Dex group compared to the IRI group (Table 3).

Table 3. Biochemistry analysis results (Arithmetic mean±standard deviation)

Group	MDA (µmol/g) in tissue	GSH (µmol/g) in tissue	OR (%95 CI)	p-value
SHAM	0.30±0.02	36.84±1.53	0.98 (0.94-1.01)	0.248
IRI	0.38±0.01[a]	29.66±1.27[a]	1.90 (0.60-6.22)	0.260
IRI&Dex	0.31±0.008[b]	35.96±1.12[b]	2.70 (0.43-17.7)	0.270

Values are presented as mean±standard deviation. Malondialdehyde (MDA) levels were significantly increased and glutathione (GSH) levels were significantly decreased in the ischemia–reperfusion injury (IRI) group compared with the SHAM group. In contrast, treatment with dexmedetomidine resulted in a significant reduction in MDA levels and a significant increase in GSH levels compared with the IRI group. Statistical analysis was performed using one-way analysis of variance (ANOVA) followed by Tukey's Honest Significant Difference (HSD) test. a $p \leq 0.05$, compared with the SHAM group, b $p \leq 0.05$, compared with the IRI group

DISCUSSION

The present study evaluated the effects of dexmedetomidine on ischemia–reperfusion–induced skeletal muscle injury in a rat model of ruptured abdominal aortic aneurysm that combines hemorrhagic shock, aortic cross-clamping, and subsequent reperfusion. Our findings demonstrate that intraperitoneal Dex administration significantly attenuated structural muscle damage, reduced apoptotic activity, and improved oxidative stress parameters when compared with untreated ischemia–reperfusion injury.

Histopathological examination revealed preserved myofibrillar architecture and nuclear morphology in the SHAM group, whereas extensive necrosis and pyknotic nuclei were observed following ischemia– reperfusion. In contrast, animals treated with Dex exhibited markedly fewer necrotic areas and a largely preserved muscle structure, indicating a protective effect against ischemic injury. These observations were further supported by immunohistochemical findings demonstrating enhanced actin and myosin expression in the Dex-treated group relative to the ischemia–reperfusion group.

Apoptosis represents a central mechanism contributing to muscle injury following prolonged ischemia and reperfusion. Caspase-3, a key effector enzyme in the apoptotic cascade, was markedly increased in the ischemia–reperfusion group, whereas Dex administration significantly reduced caspase-3 positivity, suggesting suppression of apoptosis. These findings align with previous experimental studies demonstrating that Dex mitigates apoptosis in myocardial, neural, and skeletal muscle tissues through modulation of intracellular signaling pathways [14].

Biochemical analysis further confirmed the protective effects of Dex. Malondialdehyde levels, a marker of lipid peroxidation, were significantly elevated following ischemia–reperfusion, reflecting increased oxidative stress. Dex treatment resulted in a significant reduction in MDA levels, accompanied by restoration of glutathione concentrations. These results indicate that Dex contributes to re-establishing redox balance by limiting ROS-mediated damage and preserving endogenous antioxidant defenses.

Previous experimental studies have reported comparable antioxidant and cytoprotective effects of Dex in skeletal muscle ischemia–reperfusion models, with reductions in MDA levels and preservation of antioxidant enzyme activity [15]. Clinical investigations have similarly demonstrated decreased biochemical markers of muscle injury in patients receiving Dex during tourniquet-induced ischemia or major vascular surgery [16–19]. Our findings extend this evidence by demonstrating a protective role of Dex in the context of ruptured abdominal aortic aneurysm, a clinical scenario characterized by profound ischemia and reperfusion stress affecting a large skeletal muscle mass.

The mechanisms underlying Dex-mediated protection are likely multifactorial. In addition to its sympatholytic effects, Dex has been shown to modulate inflammatory responses, inhibit mitochondrial dysfunction, and suppress apoptosis-related signaling pathways such as JAK2/STAT3 and HIF-1α [20–22]. The observed reduction in caspase-3 activation in our study supports the hypothesis that anti-apoptotic mechanisms contribute significantly to its protective effects.

Unlike many previous studies focusing on critical organs, we specifically investigated lower extremity skeletal muscle, which represents a substantial ischemic tissue burden during aortic cross-clamping. To the best of our knowledge, no experimental studies have specifically evaluated lower extremity skeletal muscle ischemia–reperfusion injury associated with ruptured abdominal aortic aneurysm. Preservation of skeletal muscle integrity may therefore play a key role in limiting systemic inflammatory response and subsequent postoperative complications.

Nevertheless, several limitations should be acknowledged. The use of a rat model may not fully replicate the complex physiological responses observed in human RAAA. Additionally, only short-term outcomes were evaluated, and functional recovery of skeletal muscle was not assessed. Furthermore, serum inflammatory markers such as IL-6 and TNF-α were not measured, which may have provided additional insight into the systemic inflammatory response. Future studies incorporating long-term follow-up, functional measurements, diverse experimental models, and comprehensive inflammatory profiling are warranted to further elucidate the clinical relevance of these findings.

CONCLUSION

In conclusion, this study demonstrates that dexmedetomidine significantly attenuates ischemia– reperfusion injury in lower extremity skeletal muscle in a rat model of ruptured abdominal aortic aneurysm. Histopathological, immunohistochemical, and biochemical findings indicate that dexmedetomidine reduces muscle damage, apoptosis, and oxidative stress when compared with untreated ischemia–reperfusion injury.

From a clinical perspective, these findings suggest that dexmedetomidine—already widely used for sedation and analgesia in perioperative and intensive care settings—may offer additional protective benefits against peripheral tissue injury during emergency aortic interventions and subsequent critical care management in patients with RAAA.

An additional distinguishing feature of this study is the intraperitoneal administration of dexmedetomidine, which represents a methodological difference from most existing studies and further underscores the experimental contribution of our findings.

Nevertheless, the limitations of this experimental study warrant cautious interpretation of the results. Further investigations involving different animal models, long-term outcome analyses, and well-designed clinical trials are required to confirm the translational relevance, efficacy, and safety of dexmedetomidine before its routine incorporation into clinical practice for the management of ischemia–reperfusion injury associated with RAAA.

Ethics Committee Approval: It was received from the Recep Tayyip Erdoğan University Animal Experiments Local Ethics Committee (Approval No: 2020/21, dated May 29, 2020).

Patient Consent for Publication: Not necessary for this manuscript.

Data Sharing Statement: The data that support the findings of this study are available from the corresponding author upon reasonable request.

Author Contributions: All authors contributed equally to the article.

Conflict of Interest: The authors declared no conflicts of interest with respect to the authorship and/or publication of this article.

Funding: The authors received Scientific Research Projects Unit of Recep Tayyip Erdoğan University (BAP ID 1174).

Acknowledgments: The authors would like to thank the Scientific Research Projects Unit of Recep Tayyip Erdoğan University for financial support.

REFERENCES

1. Visser P, Akkersdijk GJM, Blankensteijn JD. In-hospital operative mortality of ruptured abdominal aortic aneurysm: A population-based analysis of 5593 patients in the Netherlands over a 10-year period. Eur J Vasc Endovasc Surg. 2005;30:359-64.
2. Acosta S, Lindblad B, Zdanowski Z. Predictors for outcome after open and endovascular repair of ruptured abdominal aortic aneurysms. Eur J Vasc Endovasc Surg. 2007;33:277-84.
3. Lozano FS, Rodriguez JM, Garcia-Criado FJ, Barros MB, Conde PS, Gonzalez LM, et al. Postoperative evolution of inflammatory response in a model of suprarenal aortic cross-clamping with and without hemorrhagic shock: Systemic and local reactions. World J Surg. 2005;29:1248-58.
4. Wang X, Guo Z, Ding Z, Mehta JL. Inflammation, autophagy, and apoptosis after myocardial infarction. J Am Heart Assoc. 2018;7:e009.
5. Lee Y, Gustafsson ÅB. Role of apoptosis in cardiovascular disease. Apoptosis. 2009;14:536-48.
6. Porter AG, Jänicke RU. Emerging roles of caspase-3 in apoptosis. Cell Death Differ. 1999;6:99-104.
7. Zhou T, Prather ER, Garrison DE, Zuo L. Interplay between ROS and antioxidants during ischemia-reperfusion injuries in cardiac and skeletal muscle. Int J Mol Sci. 2018;19:398.
8. Uysal M. Serbest radikaller, lipit peroksitleri ve organizmada prooksidan-antioksidan dengeyi etkileyen koşullar. Klin Gelişim. 1998;11:336-41.
9. Zweier JL, Talukder MAH. The role of oxidants and free radicals in reperfusion injury. Cardiovasc Res. 2006;70:181-90.
10. Cai YE, Xu H, Yan J, Zhang L, Lu YI. Molecular targets and mechanism of action of dexmedetomidine in treatment of ischemia/reperfusion injury. Mol Med Rep. 2014;9:1542-50.
11. Géloën A, Pichot C, Leroy S, Julien C, Ghignone M, May CN, et al. Pressor response to noradrenaline in the setting of septic shock: Anything new under the sun—dexmedetomidine, clonidine? A minireview. Biomed Res Int. 2015;2015:1-8.
12. Sun J, Zheng S, Yang N, Chen B, He G, Zhu T. Dexmedetomidine inhibits apoptosis and expression of COX-2 induced by lipopolysaccharide in primary human alveolar epithelial type 2 cells. Biochem Biophys Res Commun. 2019;517:89-95.
13. Lindsay TF, Walker PM, Romaschin A. Acute pulmonary injury in a model of ruptured abdominal aortic aneurysm. J Vasc Surg. 1995;22:1-8.
14. Hemsinli D, Tumkaya L, Ergene S, Karakisi SO, Mercantepe T, Yilmaz A. Dexmedetomidine attenuates pneumocyte apoptosis and inflammation induced by aortic ischemia-reperfusion injury. Clin Exp Hypertens. 2022;44:595-600.
15. Dong X, Xing Q, Li Y, Han X, Sun L. Dexmedetomidine protects against ischemia-reperfusion injury in rat skeletal muscle. J Surg Res. 2014;186:240-45.
16. Yagmurdur H, Ozcan N, Dokumaci F, Kilinc K, Yilmaz F, Basar H. Dexmedetomidine reduces ischemia-reperfusion injury markers during upper extremity surgery with tourniquet. J Hand Surg Am. 2008;33:941-47.
17. Kundra TS, Thimmarayappa A, Dhananjaya M, Manjunatha N. Dexmedetomidine for prevention of skeletal muscle ischemia-reperfusion injury in patients with chronic limb ischemia undergoing aortobifemoral bypass surgery: A prospective double-blind randomized controlled study. Ann Card Anaesth. 2018;21:22-28.
18. Chi X, Liao M, Chen X, Zhao Y, Yang L, Luo A, et al. Dexmedetomidine attenuates myocardial injury in off-pump coronary artery bypass graft surgery. J Cardiothorac Vasc Anesth. 2016;30:44-50.
19. Li J, Zhao Y, Zhou N, Li L, Li K. Dexmedetomidine attenuates myocardial ischemia-reperfusion injury in diabetes mellitus by inhibiting endoplasmic reticulum stress. J Diabetes Res. 2019;2019:1-9.
20. Chen Y, Zhang X, Zhang B, He G, Zhou L, Xie Y. Dexmedetomidine reduces neuronal apoptosis related to cardiopulmonary bypass by inhibiting activation of the JAK2-STAT3 pathway. Drug Des Devel Ther. 2017;11:2787-96.
21. Weng X, Shi W, Zhang X, Du J. Dexmedetomidine attenuates H2O2-induced apoptosis of rat cardiomyocytes independently of antioxidant enzyme expression. Rev Port Cardiol. 2021;40:273-81.
22. Peng K, Chen WR, Xia F, Liu H, Meng XW, Zhang J, et al. Dexmedetomidine post-treatment attenuates cardiac ischaemia/reperfusion injury by inhibiting apoptosis through HIF-1α signalling. J Cell Mol Med. 2020;24:850-61.